A COMPARISON OF TWO SELF-SHIELDING MODELS ON THE ROWLANDS PIN-CELL BENCHMARK

Alain Hébert and Fréderic Fernex
DRN/DMT/SERMA/LENR
CEA Saclay
91191 Gif-sur-Yvette Cedex, France
alain.hebert@cea.fr

ABSTRACT

The paper first introduces two self-shielding models available in the APOLLO2 code: the Sanchez-Coste and the subgroup methods, the former being used for production assembly calculations. These two methods are based on mathematical and physical probability tables, respectively. A comparison study was undertaken to investigate the accuracy of these two approaches on the Rowlands pin-cell benchmark. Results indicate that both techniques lead to results consistent with Monte-Carlo reference calculations.

1. INTRODUCTION

This work was carried out with a view to validating the self-shielding algorithm of the APOLLO2 lattice code.[1] The French Atomic Energy Commission (CEA) is actively engaged in developing and using APOLLO2. Moreover, APOLLO2 is used at Électricité de France (EDF) for specific studies and is currently being evaluated for inclusion in its new cross-section generating system. It is also a component of industrial products at Framatome.

A resonance self-shielding calculation is required in any software for solving the multigroup neutron transport equation, in order to take into account the resonant behaviour of the cross sections in each energy group. A large category of resonance self-shielding models relies on probability table information in which the detailed energy-dependent cross section behaviour in each coarse energy group is replaced by its probability density representation.[2, 3, 4] We investigated two self-shielding methods based on probability tables, the first being used for production calculations in APOLLO2.

The Sanchez-Coste method consists in performing an accurate discretization of each cross-section probability density, leading to consistent probability tables. This method is not *stricto sensu* a subgroup approach, as the following two algorithms are used:[5]

- *mathematical* probability tables are used. They are obtained directly from detailed cross section information (found in the PENDF file) using a straightforward transformation.[6] Slowing-down effects are not taken into account in the calculation of the probability tables.
- an equivalent dilution is computed in each energy group for each resonant isotope and the self-shielded reaction rates are interpolated from the values tabulated by the module GROUPR in NJOY.[7]

The second method is a pure subgroup approach similar to the technique used in lattice codes HELIOS[8] and WIMS-7[9]. A set of *physical* probability tables is fitted to a set of homogeneous-domain self-shielded cross sections tabulated against dilution.[10, 11] These probability tables are subsequently used within the flux solution algorithm of the subgroup method. This method has been implemented as a *universal self-shielding* (USS) module in various lattice codes, as it is not restricted to a collision probability (CP) solution of the fine-structure function. Moreover, standard cross-section libraries can be used, as no detailed cross section information is required.

The Sanchez-Coste approach with mathematical probability tables and the USS approach with physical probability tables will be presented in the next section. A validation on the Rowlands benchmark will follow.

2. THE RESONANCE SELF-SHIELDING CALCULATION

The main problem considered in the resonance self-shielding model is how to use self-shielded cross section and probability table information, as retrieved from the isotopic cross-section library. The final objective is to evaluate $\tilde{\sigma}_{\rho,g}$, the microscopic self-shielded cross section for any reaction ρ in group g, which is formally defined as

$$\tilde{\sigma}_{\rho,g} = \mu_g \frac{\int_{u_{g-1}}^{u_g} du\ \sigma_\rho(u)\ \phi(u)}{\int_{u_{g-1}}^{u_g} du\ \phi(u)} = \mu_g \frac{\langle \sigma_\rho \phi \rangle_g}{\langle \phi \rangle_g} \tag{1}$$

where

$u_{g-1}, u_g =$ lethargy limits of group g

$\mu_g =$ SPH factor obtained from the multigroup equivalence procedure

$\phi(u) =$ neutron flux

$\sigma_\rho(u) =$ microscopic cross section for nuclear reaction ρ.

The self-shielding phenomenon is due to the following facts:

- The cross sections belonging to energy group g may include many resonances.
- Both $\sigma_\rho(u)$ and $\phi(u)$ exhibit resonant behavior with peaks and minima in opposite directions.

2.1 THE SELF-SHIELDING MODEL

Consider a CP formulation of the neutron slowing-down equation defined over a multidimensional geometry containing I regions. We will first assume that the domain contains a single resonant isotope. The scalar flux is given as

$$\phi_i(u) = \sum_{j=1}^{I} \tilde{p}_{ij}(u) \left[R_j^+ \{\phi_j(u)\} + R_j^* \{\phi_j(u)\} \right] \quad , \quad i = 1, I \quad , \tag{2}$$

where

$\phi_i(u) =$ neutron flux in sub-region i

$p_{ij}(u) =$ reduced CP for neutrons born in region i to collide in region j. The corresponding CP matrix should be computed in a closed domain (i.e., an infinite domain or a finite domain closed with reflective or periodic boundary conditions)

$R_j^+\{\phi_j(u)\} =$ slowing-down operator in region j for nuclear reactions with non-resonant isotopes

$R_j^*\{\phi_j(u)\} =$ slowing-down operator in region j for nuclear reactions with a single heavy isotope

and it is assumed that neutron sources originating from inelastic, (n,xn) and nuclear fission reactions vanish over the slowing-down energy domain.

The two slowing-down operators can be written as a function of the zero$^{\text{th}}$ Legendre moment of the differential scattering cross section $\Sigma^+_{\text{s0},j}(u \leftarrow u')$ and $\Sigma^*_{\text{s0},j}(u \leftarrow u')$ as follows:

$$R_j^+\{\phi_j(u)\} = \int_0^\infty du'\, \Sigma^+_{\text{s0},j}(u \leftarrow u')\, \phi_j(u') \tag{3}$$

and

$$R_j^*\{\phi_j(u)\} = \int_0^\infty du'\, \Sigma^*_{\text{s0},j}(u \leftarrow u')\, \phi_j(u') \quad . \tag{4}$$

We next simplify Eq. (2) by using a set of approximations proposed by Livolant and Jeanpierre.[12] The neutron flux in each region is first factorized as the product of a resonant fine-structure function $\varphi_i(u)$ with a regular distribution $\psi_i(u)$ such that

$$\phi_i(u) = \varphi_i(u)\, \psi_i(u) \quad . \tag{5}$$

The fine-structure function can be used in the definition of the effective resonance integral $I_{\rho,g}$ for nuclear reaction ρ. Calculation of these effective resonance integrals is the first step of any self-shielding procedure. They are defined as

$$I_{\rho,g} = \frac{1}{\Delta u_g} \int_{u_{g-1}}^{u_g} du\ \sigma_\rho(u)\, \varphi(u) \tag{6}$$

where $\Delta u_g = u_g - u_{g-1}$.

The microscopic self-shielded cross sections for reaction ρ in group g was defined by Eq. (1). It can now be written

$$\bar{\sigma}_{\rho,g} = \mu_g\, \frac{I_{\rho,g}}{\bar{\varphi}_g} \tag{7}$$

where $\bar{\varphi}_g$ is the averaged fine-structure function in group g, expressed as

$$\bar{\varphi}_g = \frac{1}{\Delta u_g} \int_{u_{g-1}}^{u_g} du\ \varphi(u) \quad . \tag{8}$$

Distribution $\psi_i(u)$ is called the macroscopic flux and represents the asymptotic behavior of the neutron flux between the resonances. This distribution is defined in terms of $R_i^+\{\phi_i(u)\}$, which acts as a smoothing operator on the neutron flux:

$$\psi_i(u) = \frac{1}{\Sigma_{\mathrm{s0},i}^+}\ R_i^+\{\phi_i(u)\} \tag{9}$$

where Σ_{s0,i^+} is the macroscopic scattering cross section of the non-resonant isotopes contained in region i.

The choice of the denominator is rather arbitrary. For example, the original APOLLO1 code used a different value, namely[12]

$$\psi_i(u) = \frac{1}{\Sigma_i^+}\ R_i^+\{\phi_i(u)\} \tag{10}$$

where Σ_i^+ is the macroscopic total cross section of the non-resonant isotopes contained in region i. The choice of Eq. (9) was found to be more accurate in cases where many resonant isotopes were mixed together.

The first assumption is based on the fact that the resonant isotope is heavy and that $R_i^*\{\phi_i(u)\}$, the slowing-down operator for the resonant isotope, acts over a short lethargy range. This results in

$$R_i^*\{\phi_i(u)\} = \psi_i(u)\ R_i^*\{\varphi_i(u)\} \quad . \tag{11}$$

A second approximation consists in assuming a spatially flat value for distribution $\psi_i(u)$ across the domain. The substitution of Eqs. (10) and (11) in slowing-down Eq. (2) and the simplification of the various $\psi_i(u)$ distributions leads to

$$\varphi_i(u) = \sum_{j=1}^{I} \tilde{p}_{ij}(u) \left[\Sigma_{\mathrm{s0},j}^+ + R_j^*\{\varphi_j(u)\}\right] \quad , \quad i = 1, I \quad . \tag{12}$$

At this point, we need to decide if we want to represent *distributed self-shielding effects*. The principle is to assign many sub-regions V_i to the resonant part of the geometry and to consider a fuel-to-fuel CP matrix in the self-shielding calculation. The subdivision of a fuel rod into annulus allows a more accurate representation of Plutonium build-up in the outer ring. The so-called *rim effect* is represented in Fig. (1) where we see the effect on the absorption rate distribution of using one or six fuel regions in the self-shielding calculation. Only the following lattice codes are currently capable of modelling distributed self-shielding effects: HELIOS[8], WIMS-7[9], and APOLLO2[1].

We will restrict our presentation to the more conventional case where the rim effect is not modelled. In this case, all the resonant isotopes are contained in a single sub-region with index $i = f$. In this case, the self-shielding model of Eq. (12) is simplified as follows:

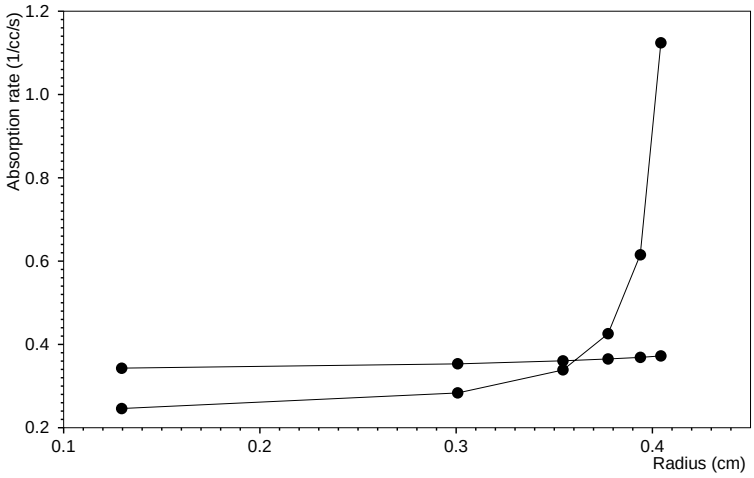

Figure 1: The rim effect.

$$\varphi_f(u) = \tilde{p}_{ff}(u)\left[\Sigma^{+}_{\mathrm{s0},f} + R^{*}_{f}\{\varphi_f(u)\}\right] + \sum_{\substack{j=1\\ j\neq f}}^{I} \tilde{p}_{fj}(u)\,\Sigma_{\mathrm{s0},j}(u) \quad . \tag{13}$$

We now introduce the *intermediate resonance* (IR) heavy slowing-down model which consists of replacing the slowing-down operator $R^{*}_{f}\{\varphi_f(u)\}$ with a linear combination of a *statistical* (ST) model[5] and a *wide resonance* (WR) model:

$$R^{*}_{f}\{\varphi_f(u)\} = \lambda_g\,\langle\Sigma^{*}_{\mathrm{s0},f}\varphi\rangle_g + (1-\lambda_g)\,\Sigma^{*}_{\mathrm{s0},f}(u)\,\varphi_f(u) \quad \text{if} \quad u_{g-1} \leq u < u_g \tag{14}$$

where

$$\langle\Sigma^{*}_{\mathrm{s0},f}\varphi_f\rangle_g = \frac{1}{\Delta u_g}\int_{u_{g-1}}^{u_g} du\;\Sigma^{*}_{\mathrm{s0},f}(u)\,\varphi_f(u) \tag{15}$$

and where λ_g is the Goldstein-Cohen parameter of the resonant isotope in group g. This parameter is set between 0 and 1. We have improved the original IR model of Goldstein and Cohen[13] by replacing the NR–WR model by the ST–WR model.

Substitution of Eq. (14) into Eq. (13) leads to

$$\varphi_f(u) = p^{\mathrm{ir}}_{ff}(u)\left[\Sigma^{+}_{\mathrm{s0},f} + \lambda_g\,\langle\Sigma^{*}_{\mathrm{s0},f}\varphi\rangle_g\right] + \sum_{\substack{j=1\\ j\neq f}}^{I} p^{\mathrm{ir}}_{fj}(u)\,\Sigma_{\mathrm{s0},j}(u) \tag{16}$$

where the scattering-reduced CPs are written

$$p^{\mathrm{ir}}_{ff}(u) = \frac{\tilde{p}_{ff}(u)}{1-(1-\lambda_g)\,\tilde{p}_{ff}(u)\,\Sigma^{*}_{\mathrm{s0},f}(u)} \;\text{ and }\; p^{\mathrm{ir}}_{fj}(u) = \frac{\tilde{p}_{fj}(u)}{1-(1-\lambda_g)\,\tilde{p}_{ff}(u)\,\Sigma^{*}_{\mathrm{s0},f}(u)} \quad . \tag{17}$$

Eq. (16) can also be written in a form where the unknown is the scattering-reduced source $Q_f^{\rm ir}(u)$:

$$\begin{aligned} Q_f^{\rm ir}(u) &= \Sigma_{{\rm s0},f}^{+} + \lambda_g \, \langle \Sigma_{{\rm s0},f}^{*} \varphi \rangle_g \\ &= \Sigma_{{\rm s0},f}^{+} + \frac{\lambda_g}{\Delta u_g} \int_{u_{g-1}}^{u_g} du' \, \Sigma_{{\rm s0},f}^{*}(u') \left\{ p_{ff}^{\rm ir}(u') \, Q_f^{\rm ir}(u') + \sum_{\substack{j=1 \\ j \neq f}}^{I} p_{fj}^{\rm ir}(u') \, \Sigma_{{\rm s0},j}(u') \right\} . \end{aligned} \tag{18}$$

The next step consists in averaging Eq. (18) over the multigroup structure of the lattice calculation. We note from this equation that $Q_f^{\rm ir}(u)$ and $\Sigma_{{\rm s0},j}(u)$ are almost constant in group g and can be extracted from the integral. We obtain

$$Q_{f,g}^{\rm ir} = \Sigma_{{\rm s0},f,g}^{+} + \lambda_g \, \langle \Sigma_{{\rm s0},f}^{*} p_{ff}^{\rm ir} \rangle_g \, Q_{f,g}^{\rm ir} + \sum_{\substack{j=1 \\ j \neq f}}^{I} \lambda_g \, \langle \Sigma_{{\rm s0},f}^{*} p_{fj}^{\rm ir} \rangle_g \, \Sigma_{{\rm s0},j,g} \tag{19}$$

where

$$\langle \Sigma_{{\rm s0},f}^{*} p_{fj}^{\rm ir} \rangle_g = \frac{1}{\Delta u_g} \int_{u_{g-1}}^{u_g} du \; \Sigma_{{\rm s0},f}^{*}(u) \, p_{fj}^{\rm ir}(u) \quad . \tag{20}$$

The most noticeable effect of this approximation is to uncouple the energy groups and to allow a simple solution of the form

$$Q_{f,g}^{\rm ir} = \frac{1}{1 - \lambda_g \, \langle \Sigma_{{\rm s0},f}^{*} p_{ff}^{\rm ir} \rangle_g} \left[\Sigma_{{\rm s0},f,g}^{+} + \sum_{\substack{j=1 \\ j \neq f}}^{I} \lambda_g \, \langle \Sigma_{{\rm s0},f}^{*} p_{fj}^{\rm ir} \rangle_g \, \Sigma_{{\rm s0},j,g} \right] \quad . \tag{21}$$

The reference self-shielded absorption rate in the heterogeneous case is computed by taking the average of the product of Eq. (16) with the lethargy-dependent absorption cross section $\sigma_{\rm a}(u)$:

$$\langle \sigma_{\rm a} \varphi_f \rangle_g^{\rm het} = \langle \sigma_{\rm a} p_{ff}^{\rm ir} \rangle_g \, Q_{f,g}^{\rm ir} + \sum_{\substack{j=1 \\ j \neq f}}^{I} \langle \sigma_{\rm a} p_{fj}^{\rm ir} \rangle_g \, \Sigma_{{\rm s0},j,g} \tag{22}$$

where

$$\langle \sigma_{\rm a} p_{fj}^{\rm ir} \rangle_g = \frac{1}{\Delta u_g} \int_{u_{g-1}}^{u_g} du \; \sigma_{\rm a}(u) \, p_{fj}^{\rm ir}(u) \quad . \tag{23}$$

2.2 LEBESGUE INTEGRATION AND PROBABILITY TABLES

The probability tables are a set of base points and weights that can be used to represent the resonant behaviour of a heavy isotope over a coarse energy grid. Here, the probability tables are introduced in the context of the IR approximation and are used to perform the integration in Eqs. (20) and (23).

The reduced CPs $p_{fj}^{\mathrm{ir}}(u)$ are a resonant function of the lethargy through the scattering-reduced total cross section of the resonant isotope, defined as

$$\sigma^{\mathrm{ir}}(u) = \sigma(u) - (1-\lambda_g)\,\sigma_{\mathrm{s0}}(u) \quad \text{if} \quad u_{g-1} \leq u < u_g \quad . \tag{24}$$

Here, we need to evaluate Riemann integrals in the form

$$\langle \sigma^{\mathrm{ir}} p_{fj}^{\mathrm{ir}} \rangle_g = \frac{1}{\Delta u_g} \int_{u_{g-1}}^{u_g} du\ \sigma^{\mathrm{ir}}(u)\, p_{fj}^{\mathrm{ir}}(u) \tag{25}$$

and

$$\langle \sigma_\rho p_{fj}^{\mathrm{ir}} \rangle_g = \frac{1}{\Delta u_g} \int_{u_{g-1}}^{u_g} du\ \sigma_\rho(u)\, p_{fj}^{\mathrm{ir}}(u) \quad . \tag{26}$$

where $\sigma_\rho(u)$ is a partial cross section which is assumed to be completely correlated to the scattering-reduced total cross section $\sigma^{\mathrm{ir}}(u)$. Eqs. (25) and (26) can therefore be replaced with Lebesgue integrals in the form

$$\langle \sigma^{\mathrm{ir}} p_{fj}^{\mathrm{ir}} \rangle_g = \int_0^{\max(\sigma^{\mathrm{ir}})} d\sigma^{\mathrm{ir}}\ \sigma^{\mathrm{ir}}\ p_{fj}^{\mathrm{ir}}(\sigma, \sigma_{\mathrm{s0}})\ \Pi(\sigma^{\mathrm{ir}}) \tag{27}$$

and

$$\langle \sigma_\rho p_{fj}^{\mathrm{ir}} \rangle_g = \int_0^{\max(\sigma^{\mathrm{ir}})} d\sigma^{\mathrm{ir}}\ \sigma_\rho(\sigma^{\mathrm{ir}})\ p_{fj}^{\mathrm{ir}}(\sigma, \sigma_{\mathrm{s0}})\ \Pi(\sigma^{\mathrm{ir}}) \tag{28}$$

where

$\Pi(\sigma^{\mathrm{ir}}) =$ probability density for the microscopic scattering-reduced total cross section $\sigma^{\mathrm{ir}}(u)$. $\Pi(\sigma^{\mathrm{ir}})d\sigma^{\mathrm{ir}}$ is the probability that the microscopic scattering-reduced total cross section of the resonant isotope will have a value between σ^{ir} and $\sigma^{\mathrm{ir}} + d\sigma^{\mathrm{ir}}$

$\sigma_\rho(\sigma^{\mathrm{ir}}) =$ average value of the microscopic partial cross section $\sigma_\rho(u)$ corresponding to the value $\sigma^{\mathrm{ir}}(u)$ of the microscopic scattering-reduced total cross section of the resonant isotope.

Eqs. (27) and (28) are then discretized with the introduction of the order K probability table $\{\omega_k,\ \sigma_k^{\mathrm{ir}},\ \sigma_{\rho,k}\ ;\ k = 1, K\}$. We obtain

$$\langle \sigma^{\rm ir} p^{\rm ir}_{fj} \rangle_g = \sum_{k=1}^{K} \sigma^{\rm ir}_k \; p^{\rm ir}_{fj}(\sigma_k, \sigma_{{\rm s}0,k}) \; \omega_k \tag{29}$$

and

$$\langle \sigma_\rho p^{\rm ir}_{fj} \rangle_g = \sum_{k=1}^{K} \sigma_{\rho,k} \; p^{\rm ir}_{fj}(\sigma_k, \sigma_{{\rm s}0,k}) \; \omega_k \quad . \tag{30}$$

The probability tables can be computed in a number of ways. The Sanchez-Coste method uses mathematical probability tables[6] whereas the USS method uses physical probability tables[11].

2.3 DETERMINATION OF THE EQUIVALENT DILUTIONS

We will now introduce the equivalence in dilution procedure, used by the Sanchez-Coste method to compute a dilution parameter, for each resonant isotope in each energy group. These dilutions will be used to interpolate self-shielded cross sections tabulated against dilution in the isotopic cross-section library. For the USS method, no equivalent dilution is required and no interpolation is made.

We first consider the scattering source term defined in Eq. (18), obtained after making Livolant-Jeanpierre approximations on the slowing-down equation for a homogeneous medium containing a single heavy isotope mixed with a non-resonant isotope. A dilution parameter $\sigma_{{\rm e},g}$ and a gamma parameter γ_g for the resonant isotope are first included in the source term:

$$q(u) = \gamma_g \; \sigma_{{\rm e},g} + \int_0^\infty du' \; \sigma_{\rm s0}(u \leftarrow u') \; \varphi(u') \tag{31}$$

so that the corresponding balance equation is similar to the equation solved in the GROUPR flux calculator of NJOY:

$$\gamma_g \; \sigma_{{\rm e},g} + \int_0^\infty du' \; \sigma_{\rm s0}(u \leftarrow u') \; \varphi(u') = \sigma(u) \; \varphi(u) + \sigma_{{\rm e},g} \; \varphi(u) \quad . \tag{32}$$

In this simple homogeneous case, the dilution and gamma parameters are respectively given as

$$\sigma_{{\rm e},g} = \frac{\Sigma^+_g}{N^*} \quad \text{and} \quad \gamma_g = \frac{\Sigma^+_{{\rm s0},g}}{\Sigma^+_g} \tag{33}$$

where N^* is the number density of the resonant isotope and where Σ^+_g and $\Sigma^+_{{\rm s0},g}$ are the macroscopic total and scattering cross sections of the non-resonant isotope in group g.

The fine-structure function for homogeneous medium is computed in module GROUPR by setting flag IWT$= -3$. $\varphi^{\rm NJOY}(u)$ is computed by assuming $\gamma = 1$. The fine-structure function for other values of γ is simply given by the relation

$$\varphi(u) = \gamma_g \; \varphi^{\rm NJOY}(u) \quad \text{if} \quad u_{g-1} \leq u < u_g \quad . \tag{34}$$

The fine-structure function for homogeneous medium is generally given as

$$\varphi(u) = \frac{q(u)}{\sigma(u) + \sigma_{\mathrm{e},g}} \quad . \tag{35}$$

Eqs. (31) and (35) can be combined with the IR heavy slowing-down model of Eq. (14). We obtain a new equation for the fine-structure function:

$$\varphi(u) = \frac{q^{\mathrm{ir}}(u)}{\sigma^{\mathrm{ir}}(u) + \sigma_{\mathrm{e},g}} \tag{36}$$

where

$$q^{\mathrm{ir}}(u) = \gamma_g \ \sigma_{\mathrm{e},g} + \lambda_g \ \langle \sigma_{\mathrm{s0}} \varphi \rangle_g \quad \text{if} \quad u_{g-1} \leq u < u_g \quad . \tag{37}$$

We next substitute Eq. (36) into Eq. (37) and take the average of the source term in group g. We obtain an expression similar to Eq. (19), given as

$$q_g^{\mathrm{ir}} = \frac{\gamma_g \ \sigma_{\mathrm{e},g}}{1 - \lambda_g \ \left\langle \dfrac{\sigma_{\mathrm{s0}}}{\sigma^{\mathrm{ir}} + \sigma_{\mathrm{e},g}} \right\rangle_g} \tag{38}$$

where

$$\left\langle \frac{\sigma_{\mathrm{s0}}}{\sigma^{\mathrm{ir}} + \sigma_{\mathrm{e},g}} \right\rangle_g = \frac{1}{\Delta u_g} \int_{u_{g-1}}^{u_g} du \ \frac{\sigma_{\mathrm{s0}}(u)}{\sigma^{\mathrm{ir}}(u) + \sigma_{\mathrm{e},g}} \quad . \tag{39}$$

Taking the derivative of the scattering source term with regard to the dilution parameter leads to

$$\frac{d}{d\sigma_{\mathrm{e},g}} \ q_g^{\mathrm{ir}} = \frac{1}{1 - \lambda_g \ \left\langle \frac{\sigma_{\mathrm{s0}}}{\sigma^{\mathrm{ir}} + \sigma_{\mathrm{e},g}} \right\rangle_g} \ \left\{ \gamma_g + q_g^{\mathrm{ir}} \ \lambda_g \ \frac{d}{d\sigma_{\mathrm{e},g}} \left\langle \frac{\sigma_{\mathrm{s0}}}{\sigma^{\mathrm{ir}} + \sigma_{\mathrm{e},g}} \right\rangle_g \right\} \quad . \tag{40}$$

The absorption rate $T_{\mathrm{a},g}$ corresponding to a given value $\sigma_{\mathrm{e},g}$ of the dilution is the average of the product of the microscopic absorption cross section and the fine-structure function given by Eq. (36):

$$T_{\mathrm{a},g} = \langle \sigma_{\mathrm{a}} \varphi \rangle_g = \left\langle \frac{\sigma_{\mathrm{a}}}{\sigma^{\mathrm{ir}} + \sigma_{\mathrm{e},g}} \right\rangle_g \ q_g^{\mathrm{ir}} \quad . \tag{41}$$

The dilution parameter $\sigma_{\mathrm{e},g}$ is set to match the absorption rate $T_{\mathrm{a},g}$ computed in the homogeneous medium with $\langle \sigma_{\mathrm{a}} \varphi_f \rangle_g^{\mathrm{het}}$, as computed by Eq. (22). This search is made using a Newton-Raphson iterative strategy in each resonant group g. Consistency will be imposed by using the *same* probability tables to compute Eqs. (20), (23), (39) and (41).

2.4 THE MULTIGROUP EQUIVALENCE PROCEDURE

Interpolation of the isotopic cross-section library with respect to the groupwise dilutions $\sigma_{\mathrm{e},g}$ or application of the USS method leads to average fine-structure functions $\langle \varphi_f \rangle_g^{\mathrm{hom}}$ and reaction rates in the form $\langle \sigma_{\rho,f}\ \varphi_f \rangle_g^{\mathrm{hom}}$. The direct self-shielded cross section for reaction ρ is defined from Eq. (1) with $\mu_g = 1$ as

$$\bar{\sigma}_{\rho,g} = \frac{\langle \sigma_{\rho,f}\ \varphi_f \rangle_g^{\mathrm{hom}}}{\langle \varphi_f \rangle_g^{\mathrm{hom}}} \quad . \tag{42}$$

These cross sections cannot be used directly in a coarse group calculation, since this type of condensation generally does not permit conservation of the reaction rates.[10] We consequently perform a multigroup equivalence procedure and introduce an SPH corrective factor for each region and coarse energy group and define equivalent cross sections by the relations:

$$\widetilde{\sigma}_{\rho,g} = \mu_{f,g}\ \bar{\sigma}_{\rho,g} \tag{43}$$

where $\mu_{f,g}$ is the SPH factor assigned to the fuel region in group g. Similarly, an SPH factor $\mu_{j,g}$ can be assigned to each non-resonant region. Note that the SPH factors are equal to 1 in homogeneous-geometry cases.

We need to compute SPH-corrected cross sections over each region and coarse energy group so as to preserve reference sources $Q_{f,g}^{\mathrm{hom}}$ and interpolated reaction rates in the form $\langle \sigma_{\rho,f}\ \varphi_f \rangle_g^{\mathrm{hom}}$. The reference sources $Q_{j,g}^{\mathrm{hom}}$ are defined as a sum of scattering rates. Their definition is arbitrary and slightly different values are used in the Sanchez-Coste and USS methods. The definition used within the Sanchez-Coste method is

$$\begin{aligned} Q_{f,g}^{\mathrm{hom}} &= \Sigma_{\mathrm{s0},f,g}^{+} + \sum_h \frac{\Delta u_h}{\Delta u_g}\ \left\langle \Sigma_{\mathrm{s0},f}^{*}\ \varphi_f \right\rangle_{g\leftarrow h}^{\mathrm{hom}} \\ \text{and}\ \ Q_{j,g}^{\mathrm{hom}} &= \Sigma_{\mathrm{s0},j,g}\ \ \text{if}\ \ j \neq f \end{aligned} \tag{44}$$

whereas the definition used within the USS method is

$$\begin{aligned} Q_{f,g}^{\mathrm{hom}} &= \Sigma_{\mathrm{s0},f,g}^{+} + \left\langle \Sigma_{\mathrm{s0},f}^{*}\ \varphi_f \right\rangle_g^{\mathrm{hom}} \\ \text{and}\ \ Q_{j,g}^{\mathrm{hom}} &= \Sigma_{\mathrm{s0},j,g}\ \ \text{if}\ \ j \neq f \quad . \end{aligned} \tag{45}$$

The same SPH factor should be used to multiply every resonant cross section belonging to each region and coarse energy group. We have chosen not to modify non-resonant cross sections mixed with resonant ones. Moreover, the corresponding homogenized fine-structure should be redefined using the relation

$$\widetilde{\varphi}_{j,g} = \frac{1}{\mu_{j,g}}\ \varphi_{j,g} \quad . \tag{46}$$

There is an intrinsic overdetermination for this type of SPH procedure when it is applied to a closed domain. An infinity of sets $\{\mu_{j,g}\ ;\ j = 1, I\}$ allows the target reaction rates to be preserved. A normalization condition should therefore be applied in each group g to determine a single solution. Here, we chose

to preserve the average fine-structure in the non-resonant sub-regions, in order to avoid any modification of the cross sections located outside the fuel. [10] We therefore write

$$\mu_{j,g} = 1 \quad ; \quad j \neq f \quad . \tag{47}$$

In each energy group g, a fixed point iteration is used to compute the SPH factor $\mu_{f,g}$. On iteration (n), the SPH-corrected fine-structure is directly obtained as

$$\tilde{\varphi}_{f,g}^{(n)} = \tilde{p}_{ff,g}^{(n-1)} \; Q_{f,g}^{\mathrm{hom}} + \sum_{\substack{j=1 \\ j \neq f}}^{I} \tilde{p}_{fj,g}^{(n-1)} \; \Sigma_{\mathrm{s0},j,g}^{+} \tag{48}$$

where the reduced CPs are computed using total cross sections corrected with the SPH factor of iteration $(n-1)$. This fixed point iteration can be accelerated by subtracting the following equation

$$p_{ff,g} \; \tilde{\Sigma}_{f,g} \; \tilde{\varphi}_{f,g} = p_{ff,g} \left[\Sigma_{f,g}^{+} \; \langle \varphi_f \rangle_g^{\mathrm{hom}} + \left\langle \Sigma_f^{*} \; \varphi_f \right\rangle_g^{\mathrm{hom}} \right] \tag{49}$$

from Eq. (48). We obtain:

$$\begin{aligned} \tilde{\varphi}_{f,g}^{(n)} \quad &= \quad \frac{1}{1 - p_{ff,g}^{(n-1)} \tilde{\Sigma}_{f,g}^{(n-1)}} \left\{ \tilde{p}_{ff,g}^{(n-1)} \; \left[Q_{f,g}^{\mathrm{hom}} - \Sigma_{f,g}^{+} \; \langle \varphi_f \rangle_g^{\mathrm{hom}} - \left\langle \Sigma_f^{*} \; \varphi_f \right\rangle_g^{\mathrm{hom}} \right] \right. \\ &+ \quad \left. \sum_{\substack{j=1 \\ j \neq f}}^{I} \tilde{p}_{fj,g}^{(n-1)} \; \Sigma_{\mathrm{s0},j,g}^{+} \right\} \end{aligned} \tag{50}$$

where $\tilde{\Sigma}_{f,g}^{(n-1)}$ is the SPH-corrected macroscopic total cross section of the fuel at iteration $(n-1)$.

The improved SPH factor is simply

$$\mu_{f,g}^{(n)} = \frac{\langle \varphi_f \rangle_g^{\mathrm{hom}}}{\tilde{\varphi}_{f,g}^{(n)}} \quad . \tag{51}$$

The iterative process is carried until convergence. Before concluding this section, a few comments can be made:

- The same quantity $\langle \varphi_f \rangle_g^{\mathrm{hom}}$ appears in the denominator of Eq. (42) and in the numerator of Eq. (51). It can therefore be simplified, as only the product of these two equations needs to be computed:

$$\widetilde{\sigma}_{\rho,g} = \frac{\left\langle \sigma_{\rho,f} \; \varphi_f \right\rangle_g^{\mathrm{hom}}}{\tilde{\varphi}_{f,g}^{(n)}} \quad . \tag{52}$$

  However, knowledge of $\langle \varphi_f \rangle_g^{\mathrm{hom}}$ is useful as an initial estimate of the flux or with the "no-sph" option of the self-shielding module.

- The interpolated fine-structure function $\langle \varphi_f \rangle_g^{\mathrm{hom}}$ is generally different from the value

$$\langle \varphi_f \rangle_g^{\mathrm{het}} = \langle p_{ff}^{\mathrm{ir}} \rangle_g \; Q_{f,g}^{\mathrm{ir}} + \sum_{\substack{j=1 \\ j \neq f}}^{I} \langle p_{fj}^{\mathrm{ir}} \rangle_g \; \Sigma_{\mathrm{s0},j,g}^{+} \tag{53}$$

  obtained from the subgroup algorithm, except in homogeneous cases.

3. NUMERICAL RESULTS

The comparisons were made for light-water reactor pin-cells without leakage. A description of this benchmark was presented by Rowlands.[14]

Two types of pin-cell were studied, one UO_2 fuelled (UOX), and the other $UPuO_2$ fuelled, the latter in two versions with different isotopic compositions (MOX–1 and MOX–2). The effects of changes in temperature and water density were also calculated in order to examine the consistency of temperature calculation methods. UOX and MOX calculations use a XMAS (172 gr) JEF 2.2 library (CEA-93 v.4 release). However, the ^{239}Pu JEF2.2 evaluation was slightly corrected before building the CEA-93 library.[15] All calculations use a ST-WR(81) heavy slowing-down model.

Four UOX cell cases were calculated: the reference case, a case with reduced water density, an isothermal temperature increase and a fuel temperature increase. The results obtained are shown in Table 1. The UOX results are obtained with a concentration of Oxygen equal to 0.033494 instead of 0.033414.

Table 1:

UOX Pin Cell Results – Cylindrical surface – Zero Buckling

	Case 1 Isothermal 293K	Case 2 Reduced H_2O density	Case 3 Fuel at 900K	Case 4 Isothermal 550K
MCNP-4A (Petten)	1.38774 $\pm$ 40 pcm	1.33452 $\pm$ 40 pcm	1.30309 $\pm$ 40 pcm	1.31492 $\pm$ 40 pcm
TRIPOLI4 (Saclay)	1.38805 $\pm$ 46 pcm	1.33585 $\pm$ 92 pcm	1.30420 $\pm$ 74 pcm	1.31792 $\pm$ 69 pcm
USS (1 rings in fuel)	1.38606 (-168 pcm)$^{(a)}$ (-199 pcm)$^{(b)}$	1.33302 (-150 pcm)$^{(a)}$ (-283 pcm)$^{(b)}$	1.30074 (-235 pcm)$^{(a)}$ (-346 pcm)$^{(b)}$	1.31545 (53 pcm)$^{(a)}$ (-247 pcm)$^{(b)}$
USS (6 rings in fuel)	1.38706 (-68 pcm)$^{(a)}$ (-99 pcm)$^{(b)}$	1.33437 (-15 pcm)$^{(a)}$ (-148 pcm)$^{(b)}$	1.30258 (-51 pcm)$^{(a)}$ (-162 pcm)$^{(b)}$	1.31704 (212 pcm)$^{(a)}$ (-88 pcm)$^{(b)}$
Sanchez-Coste (1 rings in fuel)	1.38565 (-209 pcm)$^{(a)}$ (-240 pcm)$^{(b)}$	1.33252 (-200 pcm)$^{(a)}$ (-333 pcm)$^{(b)}$	1.29976 (-333 pcm)$^{(a)}$ (-444 pcm)$^{(b)}$	1.31474 (-18 pcm)$^{(a)}$ (-318 pcm)$^{(b)}$
Sanchez-Coste (6 rings in fuel)	1.38760 (-14 pcm)$^{(a)}$ (-45 pcm)$^{(b)}$	1.33494 (42 pcm)$^{(a)}$ (-91 pcm)$^{(b)}$	1.30256 (-53 pcm)$^{(a)}$ (-164 pcm)$^{(b)}$	1.31733 (241 pcm)$^{(a)}$ (-59 pcm)$^{(b)}$

(a) Relative to MCNP. (b) Relative to TRIPOLI4.

For the two MOX cells, the effect of an increase in fuel temperature was investigated. The results obtained are shown in Table 2.

We note that TRIPOLI4 have the capability to take into account the self-shielding effects in the unresolved energy domain using mathematical probability table information. TRIPOLI4 results are therefore

Table 2:

MOX Pin Cell Results – Cylindrical surface – Zero Buckling

	Fuel 1 Isothermal 300K	Fuel 1 Fuel at 560K	Fuel 2 Isothermal 300K	Fuel 2 Fuel at 560K
MCNP-4A (Petten)	1.21840 $\pm$ 60 pcm	1.20048 $\pm$ 60 pcm	1.26106 $\pm$ 60 pcm	1.24564 $\pm$ 60 pcm
TRIPOLI4 (Saclay)	1.21935 $\pm$ 92 pcm	1.20407 $\pm$ 84 pcm	1.26088 $\pm$ 93 pcm	1.24863 $\pm$ 93 pcm
USS (1 rings in fuel)	1.21743 (-97 pcm)$^{(a)}$ (-192 pcm)$^{(b)}$	1.20191 (143 pcm)$^{(a)}$ (-216 pcm)$^{(b)}$	1.25907 (-199 pcm)$^{(a)}$ (-181 pcm)$^{(b)}$	1.24493 (-71 pcm)$^{(a)}$ (-370 pcm)$^{(b)}$
USS (6 rings in fuel)	1.21895 (55 pcm)$^{(a)}$ (-40 pcm)$^{(b)}$	1.20360 (312 pcm)$^{(a)}$ (-47 pcm)$^{(b)}$	1.26039 (-67 pcm)$^{(a)}$ (-49 pcm)$^{(b)}$	1.24642 (78 pcm)$^{(a)}$ (-221 pcm)$^{(b)}$
Sanchez-Coste (1 rings in fuel)	1.21636 (-204 pcm)$^{(a)}$ (-299 pcm)$^{(b)}$	1.20121 (73 pcm)$^{(a)}$ (-286 pcm)$^{(b)}$	1.25870 (-236 pcm)$^{(a)}$ (-218 pcm)$^{(b)}$	1.24444 (-120 pcm)$^{(a)}$ (-419 pcm)$^{(b)}$
Sanchez-Coste (6 rings in fuel)	1.21864 (24 pcm)$^{(a)}$ (-71 pcm)$^{(b)}$	1.20359 (311 pcm)$^{(a)}$ (-48 pcm)$^{(b)}$	1.26059 (-47 pcm)$^{(a)}$ (-29 pcm)$^{(b)}$	1.24646 (82 pcm)$^{(a)}$ (-217 pcm)$^{(b)}$

(a) Relative to MCNP. (b) Relative to TRIPOLI4.

considered to be more reliable. While performing the numerical tests, we also noted that the Sanchez-Coste method was numerically more stable than the USS method, the latter being very sensitive to the numerical accuracy of the Padé regression technique.[11]

CONCLUSIONS

The Rowlands pin-cell benchmark was processed using two distinct self-shielding models, implemented in the same lattice code and using the same cross-section library. The results show an acceptable agreement with reference Monte-Carlo calculations, provided that the distributed self-shielding effects in the fuel rod are correctly taken into acount. The Sanchez-Coste method was also found to be more reliable than the USS method.

ACKNOWLEDGMENTS

This work was supported by Framatome and EDF under contract EPAC–5192/CANAL–3111.

REFERENCES

1. Sanchez, R. *et al.,* "APOLLO-II: A User-Oriented, Portable, Modular Code for Multigroup Transport Assembly Calculations," *Proc. Int. Top. Mtg. Advances in Reactor Physics, Mathematics and Computation*, Paris, France, April 27-30 (1987).

2. Levitt, L. B., "The Probability Table Method for Treating Unresolved Neutron Resonances in Monte-Carlo Calculations," *Nucl. Sci. Eng.,* **49**, 450 (1972).

3. Cullen, D. E., "Application of the Probability Table Method to Multigroup Calculations of Neutron Transport," *Nucl. Sci. Eng.*, **55**, 387 (1974).

4. Nikolaev, M. N., "Comments on the Probability Table Method," *Nucl. Sci. Eng.,* **61**, 286 (1976).

5. Coste, M., "Absorption résonnante des noyaux lourds dans les réseaux hétérogènes – I-Formalisme du module d'autoprotection d'APOLLO2," Note CEA-N-2746, Commissariat à l'Énergie Atomique, France (1994).

6. Hébert, A. and Coste, M., "Computing Probability Tables for Self-Shielding Calculations in APOLLO2," *Proc. Int. Conf. on Mathematics and Computation, reactor Physics and Environmental Analysis in Nuclear Applications*, Madrid, Spain, September 27 – 30 (1999).

7. Macfarlane, R. E. and Boicourt, R. M., "NJOY, A Neutron and Photon Processing System," *Trans. Am. Nucl. Soc.*, **22**, 720 (1975).

8. Casal, J. J., Stamm'ler, R. J. J., Villarino, E. A. and Ferri, A. A., "HELIOS: Geometric Capabilities of a New Fuel-Assembly Program," *Int. Top. Mtg. Advances in Mathematics, Computation, and Reactor Physics*, Pittsburgh, Pennsylvania, April 28–May 2 (1991).

9. Halsall, M. J., "WIMS7, An Overview," *Proc. Int. Conf. on the Physics of Reactors – PHYSOR 96*, Mito, Japan, p. B-1, September 16–20 (1996).

10. Hébert, A., "Advances in the Development of a Subgroup Method for the Self-Shielding of Resonant Isotopes in Arbitrary Geometries," *Nucl. Sci. Eng.*, **126**, 245 (1997).

11. Hébert, A., "A Comparison of Three Techniques for Computing Probability Tables", *Int. Conf. on the Physics of Nuclear Science and Technology*, Long Island, New York, October 5–8 (1998).

12. Livolant, M. and Jeanpierre, F., "Autoprotection des résonances dans les réacteurs nucléaires. Application aux isotopes lourds," CEA-R-4533, Commissariat à L'Énergie Atomique, France (1974).

13. Goldstein R. and Cohen E. R., *Nucl. Sci. Eng.*, **13**, 132 (1962).

14. Rowlands, J et al, "LWR Pin Cell Benchmark Intercomparisons. An Intercomparison study organized by the JEF Project, with contributions by Britain, France, Germany, The Netherlands, Slovenia and the USA.," *JEF Report to be published* , OECD/NEA Data Bank (1999).

15. Mounier, C., "An Analysis of ^{239}Pu Evaluations in Unresolved Range", JEFF meeting, OECD, Issy-les-Moulinaux, November 29–December 1 (1999).